Investigation of Bridge and 2-Phenyl Substituent Effects on Ethylene/α-Olefin Copolymerization Behavior with 1,2′-Bridged Bis(indenyl)zirconium Dichlorides

Sarah E. Reybuck and Robert M. Waymouth*

Department of Chemistry, Stanford University, Stanford, California 94305-5080

Received September 12, 2003; Revised Manuscript Received February 2, 2004

ABSTRACT: Ethylene/propylene and ethylene/1-hexene copolymerizations were studied with a series of *ansa*-metallocenes characterized by a *gauche* orientation of the indenyl ligands: [1-(1-indenyl)-2-(2-indenyl)ethane]zirconium dichloride, Et(2-Ind)(1-Ind)$ZrCl_2$ (**1**)/MMAO, [2-(2-indenyl)-1-(2-phenyl-1-indenyl)ethane]zirconium dichloride, Et(2-Ind)(2-Ph-1-Ind)$ZrCl_2$ (**2**)/MMAO, and [(2-indenyl)(2-phenyl-1-indenyl)dimethylsilyl]zirconium dichloride, Me_2Si(2-Ind)(2-Ph-1-Ind)$ZrCl_2$ (**3**)/MMAO to determine the significance of 2-phenyl ligand substitution as well as bridge type and placement on a series of *gauche*-1,2′-bridged metallocenes. Comparison between the 1,1′-bridged metallocene *anti*-ethylenebis(1-indenyl)-zirconium dichloride and *gauche*-**1** showed that the different bridge placements gave similar copolymerization reactivity in contrast to the different reactivities observed for *anti*-1,1′-bridged dimethylsilylbis(2-phenylindenyl)zirconium dichloride and *gauche*-1,2′-dimethylsilyl-bridged **3** respectively. Similar to trends observed with unbridged systems, substitution of a phenyl group in the 2-position resulted in a significant increase in α-olefin incorporation for **2** compared to unsubstituted **1**. Ethylene-bridged **2** gave higher comonomer incorporation and a blockier comonomer distribution compared to dimethylsilylene-bridged **3**.

Introduction

Metallocene-based catalysts are of interest for both the production and study of ethylene/α-olefin copolymers. Metallocene catalyst systems have the potential to control α-olefin incorporation and distribution[1−9] in turn influencing important polymer properties such as melting behavior, flexibility, and processability.[10−16] Studies on ethylene/α-olefin copolymerization by metallocenes have shown that modifications of structural parameters such as the nature of the metal,[17] ligand substituents,[5,7,18−33] and presence of bridge[18−20,24,34−37] as well as bridge type[5,7,19,23,38,39] can influence comonomer incorporation and distribution. In general, it is reported that *ansa*-metallocenes with 1 or 2 atoms in the bridge give higher comonomer incorporation than their unbridged analogues. This observation has been explained as result of a larger coordination gap aperture for bridged compared to unbridged metallocenes allowing better accessibility for bulky α-olefin comonomers.[35] Among different bridged metallocenes, bridges giving larger coordination gap apertures generally lead to higher α-olefin incorporation.

The influence of ligand substitution on α-olefin incorporation in ethylene/α-olefin copolymerization has been less predictable than bridge effects. Contrary to steric arguments, 2-alkyl,[26,33] 2-benzyl,[26] and 2-phenyl[20,24] substituents on unbridged bis(indenyl)zirconium dichlorides give better comonomer incorporation than their unsubstituted analogues.

In the current study, the copolymerization behavior and sequence distributions for the C_1-symmetric, *gauche*-1,2′-bridged bis(indenyl) metallocenes **1**−**3** (Figure 1) activated with Akzo modified methylaluminoxane (MMAO) were investigated to determine the significance of ligand substitution as well as different bridges and bridge placement on ethylene and α-olefin selectivity with this class of metallocenes. The copolymerization reactivity ratios and sequence distributions for the *gauche*-1,2′-bridged systems are compared to those reported for the *anti*-1,1′-bridged systems *rac*-ethylenebis(1-indenyl)zirconium dichloride, *anti*-Et(1-Ind)$_2$-$ZrCl_2$, and *anti*-dimethylsilylbis(2-phenyl-1-indenyl)zirconium dichloride, *anti*-Me_2Si(2-Ph-1-Ind)$_2ZrCl_2$, the *eclipsed*-2,2′-bridged system ethylenebis(2-indenyl)zirconium dichloride, Et(2-Ind)$_2ZrCl_2$, as well as the unbridged systems bis(indenyl)zirconium dichloride, (Ind)$_2$-$ZrCl_2$, and bis(2-phenylindenyl)zirconium dichloride, (2-PhInd)$_2ZrCl_2$ (Figure 1).

Results and Discussion

Three 1,2′-bridged indenylmetallocenes were studied for their ethylene/propylene and ethylene/1-hexene copolymerization behavior: [1-(1-indenyl)-2-(2-indenyl)-ethane]zirconium dichloride, *gauche*-Et(2-Ind)(1-Ind)-$ZrCl_2$ (**1**)/MMAO, [2-(2-indenyl)-1-(2-phenyl-1-indenyl)-ethane]zirconium dichloride, *gauche*-Et(2-Ind)(2-Ph-1-Ind)$ZrCl_2$ (**2**)/MMAO, and [(2-indenyl)−(2-phenyl-1-indenyl)dimethylsilyl]zirconium dichloride, gauche-Me_2-Si(2-Ind)(2-Ph-1-Ind)$ZrCl_2$ (**3**)/MMAO. The syntheses of these complexes as well as their propylene polymerization are described elsewhere.[40]

Copolymerizations were carried out in neat α-olefin monomer with a constant overpressure of ethylene at 20 °C. Ethylene/propylene feed compositions were determined using gas fugacities as described by Kravchenko.[20] Because of the ability to access a larger range of feed ratios and comonomer incorporations using 1-hexene as a comonomer, more detailed analyses were carried out using ethylene/1-hexene as a copolymerization system. Ethylene/1-hexene feed compositions were determined using an empirical equation for ethylene solubility in 1-hexene as reported by Spitz.[41] The ethylene/propylene and ethylene/1-hexene copolymerization conditions and results are reported in Tables 1 and 2.

10.1021/ma035365t CCC: $27.50

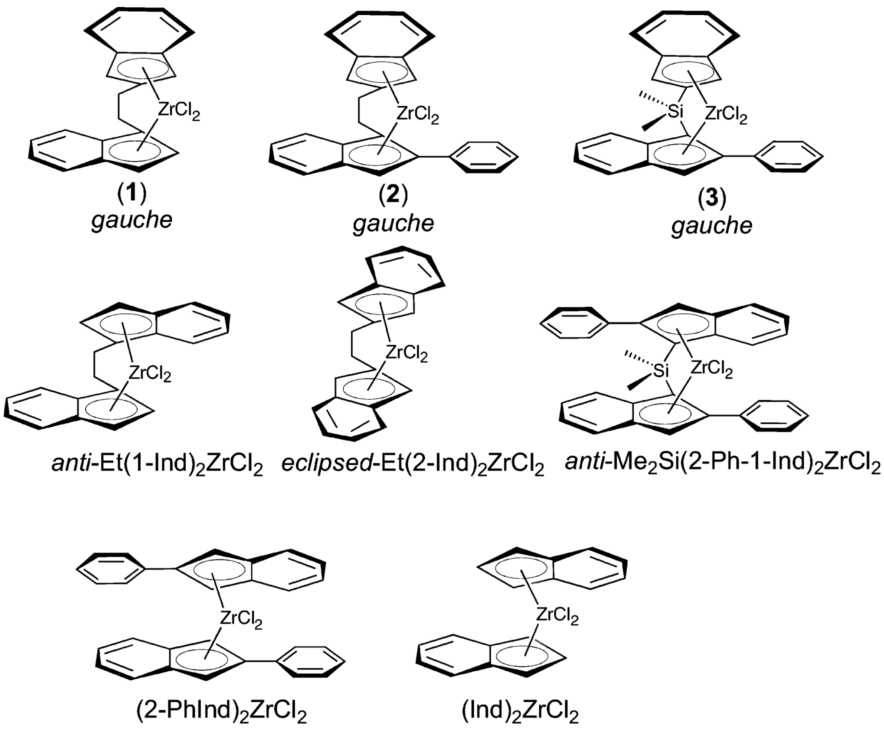

Figure 1. Structures of 1,2′-bridged metallocene complexes **1**−**3** and comparison complexes.

Table 1. Ethylene/Propylene Copolymerization with 1,2′-Bridged Metallocenes/MMAO

catal	run	[Zr] (μmol)	T_{polym} (min)	P_{total} (psig)	X_e/X_p[a] (mol/mol)	yield (g)	prod[b] (×10^3)	(E)$_{\text{copoly}}$ (mol %)	% prop conv	M_n	M_w/M_n
1	1	2.50	20	189	0.129	4.161	41.6	62.0	3.95	21 000	2.3
	2	2.50	20	164	0.087	3.393	33.9	59.7	3.38		
2	3	2.25	30	182	0.115	1.057	23.5	43.0	1.39	48 300	2.3
	4	2.25	20	167	0.091	0.279	9.3	36.1	0.40		
3	5	3.00	30	189	0.128	2.363	39.4	51.7	2.73	41 600	2.2
	6	3.00	30	170	0.091	1.225	20.4	48.0	1.50		

[a] Comonomer feed ratio. [b] Productivity = kg of polymer/(mol of Zr/h).

Table 2. Ethylene/1-Hexene Copolymerization with 1,2′-Bridged Metallocenes/MMAO

catal	run	[Zr] (μmol)	T_{polym} (min)	P_{total} (psig)	X_e/X_h[a] (mol/mol)	yield (g)	prod[b] (×10^3)	(E)$_{\text{copolymer}}$ (mol %)	% hex conv	M_n	M_w/M_n
1	1	2.5	20	198	0.3145	1.301	39.0	85.8	0.7		
	2	3.75	20	152	0.2307	3.713	74.3	83.8	2.2		
	3	2.5	20	112	0.1661	1.563	46.9	78.4	1.3	25 100	2.1
	4	2.5	30	75	0.1120	0.509	10.2	70.3	0.6		
	5	5.0	45	50	0.0783	3.646	24.3	62.4	5.1		
2	6	0.75	30	198	0.3145	2.096	139.7	78.2	1.7		
	7	3.0	40	152	0.2307	2.528	31.6	66.9	3.1		
	8	1.5	25	113	0.1676	0.253	10.0	59.5	0.4	66 200	2.6
	9	5.0	30	75	0.1120	1.287	12.9	43.6	2.7		
	10	5.0	30	50	0.0783	0.331	3.3	32.3	0.8		
3	11	0.75	30	199	0.3135	0.556	37.1	75.1	0.5		
	12	1.0	30	154	0.2341	0.232	11.6	68.6	0.3		
	13	1.0	30	112	0.1661	0.348	17.4	59.8	0.5	66 300	3.0
	14	1.5	30	77	0.1148	0.297	9.9	49.9	0.6		
	15	3.0	30	54	0.0829	0.241	4.0	42.0	0.5		

[a] Comonomer feed ratio. [b] Productivity = kg of polymer/(mol of Zr/h).

In all cases, conversions of α-olefin comonomer were kept below 5% to avoid drift in comonomer feed composition and to optimize the determination of reactivity parameters. Although these conditions are likely to lead to large uncertainties in the measured productivities, the general observation can be made that the activities for all three systems were high and decreased with increasing α-olefin comonomer in the feed.

Copolymer diad and triad distributions for ethylene/propylene were determined using ^{13}C NMR spectroscopy according to the method of Kakugo[42] and are reported in Table 3. Ethylene/1-hexene copolymer composition and sequence distributions were determined as described by Cheng[43] and are reported in Table 4.

The first-order Markov statistical model was chosen to analyze the copolymer sequence distributions.[44] According to this model, the relative reactivity toward comonomers is influenced by the identity of the last inserted monomer unit giving rise to four possible rates (Scheme 1). The reactivity ratios are defined as the rate constant of homopropagation divided by the rate constant of cross propagation: $r_e = k_{ee}/k_{ec}$, $r_c = k_{cc}/k_{ce}$ (where

Table 3. ^{13}C NMR Characterization of Ethylene/Propylene Copolymers

catal	run	mol % E	PPP	PPE	triads[a] EPE	PEP	EEP	EEE	r_e	r_p	r_er_p
1	1	62.0	0.276	0.133	0.220	0.106	0.289	0.225	10.74	0.055	0.59
	2	59.7	0.251	0.146	0.231	0.119	0.292	0.186	13.47	0.041	0.55
2	3	43.0	0.225	0.212	0.133	0.124	0.194	0.111	8.19	0.17	1.36
	4	36.1	0.290	0.235	0.115	0.128	0.175	0.057	6.73	0.18	1.21
3	5	51.7	0.062	0.142	0.279	0.199	0.207	0.110	5.31	0.06	0.33
	6	48.0	0.116	0.142	0.261	0.225	0.180	0.076	5.33	0.07	0.38

[a] Triads do not sum to 1.00 for all runs. This reflects the experimental error in the calculation of the triads from ^{13}C NMR.

Table 4. ^{13}C NMR Characterization of Ethylene/1-Hexene Copolymers

catal	run	mol % E	HHH	HHE	triads[a] EHE	HEH	EEH	EEE	r_e	r_h	r_er_h
1	1	85.8	0.000	0.015	0.127	0.013	0.217	0.613	17.1	0.017	0.30
	2	83.8	0.000	0.018	0.144	0.027	0.264	0.556	19.5	0.014	0.27
	3	78.4	0.000	0.046	0.170	0.050	0.292	0.441	18.3	0.020	0.36
	4	70.3	0.024	0.073	0.200	0.072	0.307	0.328	18.2	0.029	0.52
	5	62.4	0.022	0.145	0.209	0.096	0.298	0.225	17.0	0.026	0.44
2	6	78.2	0.035	0.052	0.131	0.022	0.261	0.501	12.8	0.122	1.57
	7	66.9	0.078	0.114	0.140	0.048	0.261	0.354	10.7	0.158	1.68
	8	59.5	0.142	0.133	0.131	0.065	0.268	0.263	12.0	0.177	2.12
	9	43.6	0.248	0.195	0.121	0.075	0.203	0.153	10.4	0.177	1.84
	10	32.3	0.390	0.202	0.085	0.089	0.159	0.076	10.7	0.207	2.21
3	11	75.1	0.032	0.040	0.178	0.060	0.278	0.422	9.0	0.083	0.75
	12	68.6	0.062	0.059	0.193	0.072	0.275	0.343	9.2	0.097	0.89
	13	59.8	0.075	0.136	0.191	0.109	0.245	0.228	8.1	0.091	0.74
	14	49.9	0.154	0.164	0.183	0.120	0.222	0.154	8.7	0.102	0.89
	15	42.0	0.235	0.193	0.153	0.129	0.183	0.103	9.4	0.110	1.03

[a] Triads do not sum to 1.00 for all runs. This reflects the experimental error in the calculation of the triads from ^{13}C NMR.

Scheme 1. First-Order Markov Model for Olefin Copolymerization

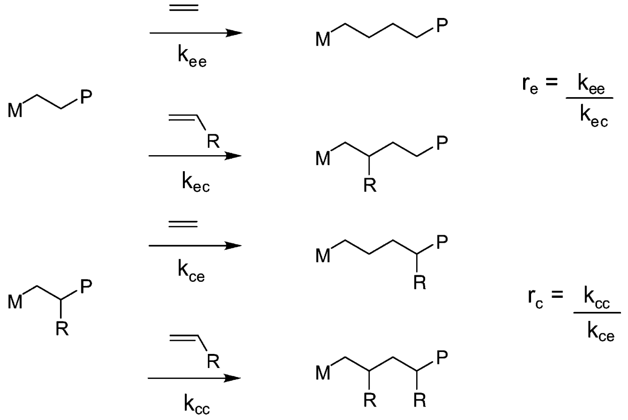

k_{xy} is defined as the rate of insertion of monomer y given the previous insertion of monomer x; e = ethylene, c = comonomer).

Reactivity ratios were determined from the triads for each individual run according to the following two equations:[45]

$$r_e = \frac{(2[\mathrm{EEE}] + [\mathrm{EEC}])}{(2[\mathrm{ECE}] + [\mathrm{CCE}])\dfrac{X_e}{X_c}}$$

$$r_c = \frac{(2[\mathrm{CCC}] + [\mathrm{CCE}])\dfrac{X_e}{X_c}}{(2[\mathrm{ECE}] + [\mathrm{CCE}])}$$

Average reactivity ratios and their standard deviations are reported in Table 5.

For ethylene/propylene and ethylene/1-hexene copolymerizations with all three systems, $r_e > 1$ while $r_c < 1$, indicating a preference for ethylene insertion compared to α-olefin. For the unsubstituted system **1**, r_e values are higher and r_c values are lower for E/H compared to E/P. This trend is similar to that observed for many metallocene systems and could be explained by the increased steric bulk of 1-hexene compared to propylene.

***Ansa* Effect: Et vs Me$_2$Si Bridge.** The effect of different bridges on copolymerization with the 1,2′-bridged systems can be evaluated by comparing ethylene-bridged complex **2** and dimethylsilyl-bridged complex **3**. The nature of the bridge influences both the geometrical and electronic properties of the metallocene.[46] The type of bridge appeared to have little influence on copolymer molecular weight as both **2** and **3** showed similar weights and narrow polydispersities.

The 1,2′-bridged metallocenes showed r_e values increasing in the order **3** < **2** < **1**. The ethylene-bridged metallocene, **2**, showed the highest r_h resulting in a product of reactivity ratios slightly greater than 1 ($r_er_h = 1.9 \pm 0.3$). The first-order Markov model describes comonomer reactivity as dependent upon the identity of the last inserted monomer unit (see Scheme 1). When ethylene is the last inserted unit, the selectivity toward another ethylene insertion is described by r_e (k_{ee}/k_{eh}). Selectivity toward ethylene following 1-hexene as the last inserted unit is described by $1/r_h$ (k_{he}/k_{hh}). The relatively high value of r_h for metallocene **2** is unusual in that it implies that the selectivity for ethylene insertion following an ethylene insertion ($r_e = k_{ee}/k_{eh} = 11$) is higher than that following a 1-hexene insertion ($1/r_h = k_{he}/k_{hh} = 5.9$). This is opposite the trend observed for most metallocenes (including **1**,**3**, and others in Tables 6 and 7 where $1/r_h > r_e$) and opposite what might be predicted on steric grounds, since one would expect that a branched polymer chain would lead to a higher preference for ethylene insertion relative to an unbranched chain.

One possible explanation for this unusual behavior of complex **2** is based on the conformational flexibility observed for ethylene bridged metallocenes. Studies by Brintzinger[47] and by Piemontesi[48] have shown that for

Table 5. Average Reactivity Ratios for Ethylene/1-Hexene Copolymerizations

catal	N_{exp}[a]	X_e/X_h[b]	% E in polymer[c]	r_e[d,e]	r_h[d,e]	r_er_h[d,e]	r_h/r_e ($\times 10^5$)
1	5	0.08−0.31	62−86	18 ± 1	0.021 ± 0.006	0.4 ± 0.1	120 ± 40
2	5	0.08−0.31	32−78	11 ± 1	0.17 ± 0.03	1.9 ± 0.3	1500 ± 400
3	5	0.08−0.31	42−75	8.9 ± 0.5	0.10 ± 0.01	0.9 ± 0.1	1100 ± 100

[a] Number of experiments used for determination of the average reactivity ratios. [b] Range of the ratios of mole fractions of ethylene and 1-hexene in the monomer feed. [c] Range of mol % E in the copolymers as determined by ^{13}C NMR. [d] Calculated as the average over all runs (av $\pm \sigma$). [e] Standard deviation calculated as $\sigma = [(1/(N-1))\Sigma(r_{e,h,\ eh,\ h/e(exp)} - r_{e,h,\ eh,\ h/e(av)})^2]^{1/2}$ where $r_{e,h,\ eh,\ h/e(exp)}$ is the reactivity ratio calculated for the triads of an individual run and $r_{e,h,\ eh,\ h/e(av)}$ is the average reactivity ratio.

Table 6. Influence of 2-Phenyl Substitution on Ethylene/1-Hexene Copolymerization Parameters

catal	N_{exp}	T (°C)	mol % E in polymer	r_e	r_h	r_er_h	M_n ($\times 10^3$)	M_w/M_n	ref
Et(2-Ind)(1-Ind)ZrCl$_2$ (**1**)	5	20	62−86	18 ± 1	0.021 ± 0.006	0.4 ± 0.1	25.1 (78.4% E)	2.1	this work
Et(2-Ind)(2-Ph-1-Ind)ZrCl$_2$ (**2**)	5	20	32−78	11 ± 1	0.17 ± 0.03	1.9 ± 0.3	66.2 (59.5% E)	2.6	this work
(Ind)$_2$ZrCl$_2$	5	20	76−89	149 ± 23	0.004 ± 0.006	0.5 ± 0.9	196.8 (78.8% E)	2.5	24
(2-PhInd)$_2$ZrCl$_2$	5	20	39−67	8 ± 1	0.09 ± 0.01	0.7 ± 0.1	365.3 (61.8% E)	3.2	24

Table 7. Influence of Bridge Position on Ethylene/α-Olefin Copolymerization Parameters

catal	α-olefin	T (°C)	mol % E in polymer	r_e	r_c	r_er_c	M_n ($\times 10^3$)	M_w/M_n	ref
anti-Et(1-Ind)$_2$ZrCl$_2$	C$_6$	20	53−81	14 ± 2	0.027 ± 0.008	0.4 ± 0.1	25.0 (66.7% E)	2.3	24
gauche-Et(2-Ind)(1-Ind)ZrCl$_2$ (**1**)	C$_6$	20	62−86	18 ± 1	0.021 ± 0.006	0.4 ± 0.1	25.1 (78.4% E)	2.1	this work
eclipsed-Et(2-Ind)$_2$ZrCl$_2$	C$_6$	70	96−99	182−235	n.d.[a]	n.d.	8.5 (90.1% E)	2.6	51
anti-Me$_2$Si(2-Ph-1-Ind)$_2$ZrCl$_2$	C$_3$	20	34−38	2.6 ± 0.2	0.20 ± 0.01	0.53	17.4 (34% E)	3.8	50
gauche-Me$_2$Si (2-Ind)(2-Ph-1-Ind)ZrCl$_2$ (**3**)	C$_3$	20	48−52	5.3	0.065	0.3	41.6 (51.7% E)	2.2	this work

[a] No adjacent 1-hexene units were detectable, and so r_h and r_er_h were not calculated.

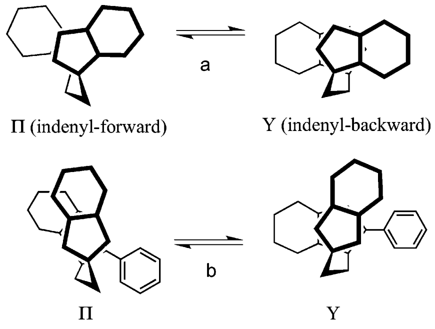

Figure 2. Ethylene-bridged bis(indenyl) complex ligand conformations.

ethylene-bridged metallocenes such as *anti*-Et(1-Ind)$_2$ZrCl$_2$, there is rapid interconversion between two conformations, indenyl-forward and indenyl-backward, at room temperature (Figure 2a). Computational studies by Pakkanen[49] have shown that substituents such as siloxy groups on the 2-position of the indenyl ligands can play a role in determining the preferred conformation for neutral metallocene dichloride complexes. Similar conformational flexibility may also be possible for 1,2′-ethylene-bridged complexes (Figure 2b). The steric influence of the phenyl substituent and last inserted bulky comonomer, coupled with the conformationally flexible ethylene bridge, may give rise to preferential stabilization of the Y conformation for **2** at a hexene-terminated chain, leading to a more accessible conformation for a subsequent 1-hexene insertion.[50,51]

Effect of Phenyl Substitution. Previous studies by our group found that introduction of a 2-substituent, particularly a 2-phenyl substituent, in a series of unbridged bis(indenyl) zirconium dichlorides resulted in a significant increase in comonomer incorporation in ethylene/1-hexene copolymerization compared to the unsubstituted metallocene (Ind)$_2$ZrCl$_2$.[24] One explanation postulated by that study was that steric interaction between the two phenyl groups decreased the accessibility of conformations in which the indenyl ligands crowded the metallocene's coordination sites (such as gauche conformations), thus making the metallocene more likely to adopt conformations in which the coordination sites were more open for 1-hexene coordination.[24]

In the current study, a similar increase in α-olefin incorporation upon substitution of the indenyl ligand with a phenyl group is observed for the gauche 1,2′-bridged systems. Substitution of a phenyl group in the 2-position, as with complex **2**, results in much higher propylene and 1-hexene incorporation compared to the unsubstituted system **1**. Phenyl substitution also affected copolymer molecular weight as both phenyl substituted complexes **2** and **3** afforded higher molecular weights than those from the unsubstituted complex **1**.

A comparison of ethylene/1-hexene copolymerization parameters for the 1,2′-bridged and unbridged systems is presented in Table 6. In contrast to the unbridged systems, in which higher 1-hexene incorporation results from both lower r_e and higher r_h for (2-PhInd)$_2$ZrCl$_2$ compared to (Ind)$_2$ZrCl$_2$, higher 1-hexene incorporation for **2** compared to **1** results primarily from a much higher r_h (by almost an order of magnitude) while r_e only decreases slightly. Higher 1-hexene incorporation and higher concentration of HHH homosequences for complex **2** (see Table 4) may be due to the combined steric effects of the phenyl substituent and previously inserted 1-hexene unit influencing the conformation of the active species to be more accessible to further 1-hexene insertions.

Thus, our previous hypothesis for the unbridged systems—that a 2-phenyl substituent results in higher 1-hexene incorporation as a consequence of biasing the conformational dynamics[24]—cannot fully explain the similar increase in comonomer incorporation for the more stereorigid *ansa*-metallocenes. We suspect that subtle electronic effects caused by an attached aryl substituent that is conjugated to the indenyl ligand may also lead to higher hexene incorporation. We note that higher comonomer incorporation has also been observed for bridged 4-phenylindenyl[7] and benzannelated[27] zirconocenes. These results suggest that conformational hypotheses cannot be the sole origin of the higher comonomer selectivities of 2-aryl-substituted systems relative to the indenyl complexes,[24] but the origin of this “conjugated arene” effect is still not well understood.

Effect of Bridge Position. The effect of different bridge placement (*anti*-1,1′ vs *gauche*-1,2′ bridge) on copolymerization selectivity among zirconocenes with a bis(indenyl) ligand framework is revealed by comparing the g*auche*-1,2′-dimethylsilyl-bridged, 2-phenyl-substituted complex **3** and the previously reported 1,1′-bridged *anti*-$Me_2Si(2\text{-}Ph\text{-}1\text{-}Ind)_2ZrCl_2$ (Figure 1).[52] These results shows that the *anti*-1,1′-bridged complex has higher selectivity toward 1-hexene compared to the *gauche*-1,2′-bridged complex. These results indicate that changing bridge placement and thus ligand environment can influence the comonomer reactivity. Nevertheless, this trend was not consistent for all types of bridging units in that the *anti*-$Et(1\text{-}Ind)_2ZrCl_2$ showed similar copolymerization behavior to the *gauche*-1,2′-bridged complex **1** (Table 7). Despite their different coordination geometries, copolymers from these two metallocenes show very similar reactivity ratios as well as copolymer molecular weights.

Additional insight into the effect of variations in bridge position is possible by examining the copolymerization results for *eclipsed*-$Et(2\text{-}Ind)_2ZrCl_2$ reported by Schaverien and co-workers[53] (Figure 1, Table 7). In contrast to the relatively high α-olefin incorporation observed for the *anti*-1,1′ and *gauche*-1,2′-ethylene-bridged bis(indenyl) complexes, the *eclipsed*-2,2′-bridged system shows very low selectivity for 1-hexene incorporation.

Conclusions

Ethylene/α-olefin copolymerizations with a series of 1,2′-bridged metallocenes were investigated and compared to results reported for 1,1′- and 2,2′-bridged complexes to determine the influence of ligand substitution as well as bridge type and placement on comonomer incorporation and distribution. Comparison between results for the phenyl-substituted complexes **2** and **3** with ethylene and dimethylsilyl bridges respectively showed that the nature of the bridge has a significant effect on both the incorporation and sequence distribution of the α-olefin. Substitution of a phenyl group at the 2-position of the indene in complex **2** gave this metallocene a significant increase in α-olefin incorporation as well as enhancement of α-olefin homosequences as compared to unsubstituted **1**. The effects of the different bridges and the phenyl substituent on comonomer incorporation and distribution may be at least partially explained by a combination of the steric effects of the phenyl substituent and previously inserted α-olefin unit coupling with the flexibility of the ethylene bridge to give conformations of the active species in which once one bulky α-olefin inserts, the active species becomes more accessible to further α-olefin insertion. Despite their different coordination geometries, 1,1′- and 1,2′-bridged unsubstituted complexes **1** and *anti*-$Et(1\text{-}Ind)_2ZrCl_2$ showed very similar copolymerization behavior in contrast to results for dimethylsilyl-bridged complexes which show higher incorporation for the *anti*-1,1′-bridged ligand geometry.

Experimental Section

General Considerations. Schlenk techniques and a Vacuum Atmospheres drybox were used in handling air- and moisture-sensitive compounds. The catalyst precursors **1**, **2**, and **3** were prepared according to the previously described procedures.[40] Polymerization grade ethylene (supplied by Matheson), liquid propylene (supplied by Scott Specialty Gases), and toluene were purified by passage through columns containing Q5 and alumina. Modified methylaluminoxane (MMAO Type 4) was supplied as a toluene solution by Akzo Nobel (6.9% v/v) and dried under vacuum to remove solvent and residual trimethylaluminum prior to use. 1-Hexene (97%) was obtained from Aldrich and was dried over sodium, distilled, and degassed prior to use.

Polymerizations were carried out in a 300 mL stainless steel Parr reactor equipped with a mechanical stirrer. The temperature was maintained at 20 °C via an ethylene glycol/water cooling loop.

Ethylene/Propylene Copolymerizations. The Parr reactor was evacuated on a vacuum line for at least 30 min and then filled with the desired overpressure of ethylene. The reactor was vented to 10 psig and then flushed three times with 100 psig of propylene. After venting the reactor to 10 psig, a solution of 100 mg of MMAO in 18 mL of toluene (prepared in the drybox) in a 150 mL double-ended injection tube was injected under propylene pressure. Liquid propylene (100 mL) was condensed into a sight glass and transferred into the reactor. The ethylene gas was reconnected, and the reactor was stirred for at least 30 min. The metallocene stock solution was prepared by dissolving 4−7 mg of the metallocene in 25 mL of toluene. The desired amount of metallocene stock solution was diluted to 2 total mL of toluene and loaded into a 25 mL double-ended injection tube. The polymerization was started by disconnecting the ethylene feed, stopping stirring, venting 5 psig, injecting the metallocene solution under ethylene pressure, reconnecting the ethylene feed, and starting stirring. After the appropriate polymerization time, the polymerization was quenched with 15 mL of methanol pressurized under argon. The reactor contents were stirred in acidified methanol overnight. After filtering and washing with additional methanol, the polymers were dried in a 40 °C vacuum oven for at least 6 h. Conversions of propylene were kept below 5% to ensure an approximately constant comonomer feed. Polymer yields were kept below 5 g to avoid mass transfer limitations. Comonomer feed composition in the liquid phase was determined using fugacity diagrams.[20]

Ethylene/Hexene Copolymerizations. The reactor was evacuated for at least 30 min on a vacuum line and then refilled and flushed three to four times with ethylene. MMAO (100 mg) was suspended in 35 mL of 1-hexene in a drybox and loaded into a 150 mL double-ended injection tube. This MMAO/1-hexene suspension was injected into the reactor and allowed to equilibrate under the appropriate ethylene pressure while stirring for at least 30 min. The metallocene stock solution was prepared by dissolving 4−7 mg of the metallocene in 25 mL of toluene. The desired amount of the stock solution, typically 10−100 μL, was diluted into 5 mL of 1-hexene and loaded into a 25 mL double-ended injection tube. The polymerization was started by disconnecting the ethylene feed, venting the reactor by 10 psig, injecting the metallocene solution under ethylene pressure, and finally reconnecting the ethylene feed. The polymerization temperature was controlled using an ethylene glycol/water cooling loop. After the desired reaction time, the ethylene feed was disconnected, and 15 mL of methanol was injected into the reactor. The contents of the reactor were poured into acidified methanol and stirred overnight. After filtering and washing with additional methanol, the polymers were dried for at least 6 h in a 40 °C vacuum oven. Conversions of hexene comonomer were kept below 6% and copolymer yields were kept below 4 g.

Polymer Analysis. $^{13}C\{^1H\}$ NMR spectra were recorded using a Varian Inova 300 MHz NMR (75 MHz resolution for $^{13}C\{^1H\}$ NMR) equipped with a 10 mm broad-band probe. Polymer samples (150 mg) were run in a 90:10 v/v solution of

1,2-dichlorobenzene/benzene-d_6 containing approximately 5 mg of chromium(III) acetylacetonate to reduce T_1. Spectra were recorded using pulse repetition intervals of 5 s and gated proton decoupling. High-temperature GPC was performed at BP on a Waters 150C GPC at 139 °C in 1,2,4-trichlorobenzene with two Polymer Laboratories PL GEL Mixed-B columns at a flow rate of 1 mL/min. HDPE standards were used.

Acknowledgment. Financial support from the NSF (CHE-9910240, CHE-0305436), BP, and an Althouse Family Stanford Graduate Fellowship to S.E.R. are gratefully acknowledged. We thank David McFarland of BP for polymer GPC analysis.

References and Notes

(1) Uozumi, T.; Miyazawa, K.; Sano, T.; Soga, K. *Macromol. Rapid Commun.* **1997**, *18*, 883−889.
(2) Uozumi, T.; Ahn, C. H.; Tomisaka, M.; Jin, J.; Tian, G.; Sano, T.; Soga, K. *Macromol. Chem. Phys.* **2000**, *201*, 1748−1752.
(3) Arndt, M.; Kaminsky, W.; Schauwienold, A. M.; Weingarten, U. *Macromol. Chem. Phys.* **1998**, *199*, 1135−1152.
(4) Leclerc, M. K.; Waymouth, R. M. *Angew. Chem., Int. Ed. Engl.* **1998**, *37*, 922−925.
(5) Fan, W.; Leclerc, M. K.; Waymouth, R. M. *J. Am. Chem. Soc.* **2001**, *123*, 9555−9563.
(6) Galimberti, M.; Piemontesi, F.; Fusco, O.; Camurati, I.; Destro, M. *Macromolecules* **1998**, *31*, 3409−3416.
(7) Galimberti, M.; Piemontesi, F.; Mascellani, N.; Camurati, I.; Fusco, O.; Destro, M. *Macromolecules* **1999**, *32*, 7968−7976.
(8) Galimberti, M.; Piemontesi, F.; Fusco, O. In *Metallocene-Based Polyolefins*; Scheirs, J.; Kaminsky, W., Eds.; Wiley: Chichester, England, 2000; Vol. 1, pp 309−343.
(9) Hung, J.; Waymouth, R. M. *Macromolecules* **2003**, *36*, 2454−2463.
(10) Alamo, R. G.; Mandelkern, L. *Thermochim. Acta* **1994**, *238*, 155−201.
(11) Burfield, D. R. *Macromolecules* **1987**, *20*, 3020−3023.
(12) Simanke, A. G.; Galland, G. B.; Freitas, L.; daJornada, J. A. H.; Quijada, R.; Mauler, R. S. *Polymer* **1999**, *40*, 5489−5495.
(13) Simanke, A. G.; Galland, G. B.; Neto, R. B.; Quijada, R.; Mauler, R. S. *J. Appl. Polym. Sci.* **1999**, *74*, 1194−1200.
(14) Schulze, U.; Arndt, M.; Freidanck, F.; Beulich, I.; Pompe, G.; Meyer, E.; Jehnichen, D.; Pionteck, J.; Kaminsky, W. *J. Macromol. Sci., Pure. Appl. Chem.* **1998**, *A35*, 1037−1044.
(15) Xu, X. R.; Xu, J. T.; Feng, L. X.; Chen, W. *J. Appl. Polym. Sci.* **2000**, *77*, 1709−1715.
(16) Brintzinger, H. H.; Fischer, D.; Mulhaupt, R.; Rieger, B.; Waymouth, R. M. *Angew. Chem., Int. Ed. Engl.* **1995**, *34*, 1143−1170.
(17) Koivumaki, J. *Polym. Bull. (Berlin)* **1995**, *34*, 413−418.
(18) Chien, J. C. W.; He, D. W. *J. Polym. Sci., Part A: Polym. Chem.* **1991**, *29*, 1585−1593.
(19) Karol, F. J.; Kao, S. C.; Wasserman, E. P.; Brady, R. C. *New J. Chem.* **1997**, *21*, 797−805.
(20) Kravchenko, R.; Waymouth, R. M. *Macromolecules* **1998**, *31*, 1−6.
(21) Harkki, O.; Lehmus, P.; Leino, R.; Luttikhedde, H. J. G.; Nasman, J. H.; Seppala, J. V. *Macromol. Chem. Phys.* **1999**, *200*, 1561−1565.
(22) Lehmus, P.; Kokko, E.; Harkki, O.; Leino, R.; Luttikhedde, H. J. G.; Nasman, J. H.; Seppala, J. V. *Macromolecules* **1999**, *32*, 3547−3552.
(23) Lehmus, P.; Harkki, O.; Leino, R.; Luttikhedde, H. J. G.; Nasman, J. H.; Seppala, J. V. *Macromol. Chem. Phys.* **1998**, *199*, 1965−1972.
(24) Reybuck, S. E.; Meyer, A.; Waymouth, R. M. *Macromolecules* **2002**, *35*, 637−643.
(25) Yano, A.; Hasegawa, S.; Kaneko, T.; Sone, M.; Sato, M.; Akimoto, A. *Macromol. Chem. Phys.* **1999**, *200*, 1542−1553.
(26) Yoon, J. S.; Lee, D. H.; Park, E. S.; Lee, I. M.; Park, D. K.; Jung, S. O. *J. Appl. Polym. Sci.* **2000**, *75*, 928−937.
(27) Schneider, M. J.; Suhm, J.; Mulhaupt, R.; Prosenc, M. H.; Brintzinger, H. H. *Macromolecules* **1997**, *30*, 3164−3168.
(28) Mohring, P. C.; Coville, N. J. *J. Mol. Catal. A: Chem.* **1995**, *96*, 181−195.
(29) Yano, A.; Sone, M.; Yamada, S.; Hasegawa, S.; Sato, M.; Akimoto, A. *J. Mol. Catal. A: Chem.* **2000**, *156*, 133−141.
(30) Yano, A.; Sone, M.; Yamada, S.; Hasegawa, S.; Akimoto, A. *Macromol. Chem. Phys.* **1999**, *200*, 917−923.
(31) Suhm, J.; Schneider, M. J.; Mulhaupt, R. *J. Mol. Catal. A: Chem.* **1998**, *128*, 215−227.
(32) Wigum, H.; Tangen, L.; Stovneng, J. A.; Rytter, E. *J. Polym. Sci., Part A: Polym. Chem.* **2000**, *38*, 3161−3172.
(33) van Beek, J. A.; de Vries, J. G.; Arts, H. J.; Persad, R.; van Doremaele, G. H. J. U.S. Patent 5646322, 1997.
(34) Quijada, R.; Dupont, J.; Miranda, M. S. L.; Scipioni, R. B.; Galland, G. B. *Macromol. Chem. Phys.* **1995**, *196*, 3991−4000.
(35) Quijada, R.; Scipioni, R. B.; Mauler, R. S.; Galland, G. B.; Miranda, M. S. L. *Polym. Bull. (Berlin)* **1995**, *35*, 299−306.
(36) Zambelli, A.; Grassi, A.; Galimberti, M.; Mazzocchi, R.; Piemontesi, F. *Makromol. Chem., Rapid Commun.* **1991**, *12*, 523−528.
(37) Lehtinen, C.; Lofgren, B. *Eur. Polym. J.* **1997**, *33*, 115−120.
(38) Kim, I.; Kim, S. Y.; Lee, M. H.; Do, Y.; Won, M. S. *J. Polym. Sci., Part A: Polym. Chem.* **1999**, *37*, 2763−2772.
(39) Koppl, A.; Babel, A. I.; Alt, H. G. *J. Mol. Catal. A: Chem.* **2000**, *153*, 109−119.
(40) Finze, M.; Reybuck, S. E.; Waymouth, R. M. *Macromolecules* **2003**, *36*, 9325−9334.
(41) Spitz, R.; Florin, B.; Guyot, A. *Eur. Polym. J.* **1979**, *15*, 441−444.
(42) Kakugo, M.; Naito, Y.; Mizunuma, K.; Miyatake, T. *Macromolecules* **1982**, *15*, 1150−1152.
(43) Cheng, H. N. *Polym. Bull. (Berlin)* **1991**, *26*, 325−332.
(44) Odian, J. *Principles of Polymerization*, 3rd ed.; John Wiley and Sons: New York, 1991.
(45) Fink, G.; Richter, W. J. *Polymer Handbook*, 4th ed.; Wiley: New York, 1999; Vol. II.
(46) Zachmanoglou, C. E.; Docrat, A.; Bridgewater, B. M.; Parkin, G.; Brandow, C. G.; Bercaw, J. E.; Jardine, C. N.; Lyall, M.; Green, J. C.; Keister, J. B. *J. Am. Chem. Soc.* **2002**, *124*, 9525−9546.
(47) Brintzinger, H. H. *Transition Metals and Organometallics as Catalysts for Olefin Polymerization*; Springer-Verlag: Berlin, 1988.
(48) Piemontesi, F.; Camurati, I.; Resconi, L.; Balboni, D.; Sironi, A.; Moret, M.; Zeigler, R.; Piccolrovazzi, N. *Organometallics* **1995**, *14*, 1256−1266.
(49) Linnolahti, M.; Pakkanen, T. A.; Leino, R.; Luttikhedde, H. J. G.; Wilen, C. E.; Nasman, J. H. *Eur. J. Inorg. Chem.* **2001**, 2033−2040.
(50) A reviewer has pointed out that r_h appears to increase as the 1-hexene content in the polymers increase for complexes 1−3 (Table 4). This slight increase in r_h occurs as the total monomer concentration decreases and may be a consequence of a competitive processes at lower monomer concentrations (such as conformational dynamics (Figure 2) or chain "back-skip"),[51] but further studies are required to determine the origin of these trends.
(51) Mohammed, J.; Nele, M.; Al-Humydi, A.; Xin, S.; Stapleton, R. A.; Collins, S. *J. Am. Chem. Soc.* **2003**, *125*, 7930−7941.
(52) Dankova, M.; Kravchenko, R. L.; Cole, A. P.; Waymouth, R. M. *Macromolecules* **2002**, *35*, 2882−2891.
(53) Schaverien, C. J.; Ernst, R.; Schut, P.; Dall'Occo, T. *Organometallics* **2001**, *20*, 3436−3452.

MA035365T